# Thresholds for Activation of Rabbit Retinal Ganglion Cells with an Ultrafine, Extracellular Microelectrode

*Ralph J. Jensen,*[1] *Joseph F. Rizzo III,*[1,2] *Ofer R. Ziv,*[1,3] *Andrew Grumet,*[3] *and John Wyatt*[3]

**Purpose.** To determine electrical thresholds required for extracellular activation of retinal ganglion cells as part of a project to develop an epiretinal prosthesis.

**Methods.** Retinal ganglion cells were recorded extracellularly in retinas isolated from adult New Zealand White rabbits. Electrical current pulses of 100-$\mu$s duration were delivered to the inner surface of the retina from a 5-$\mu$m long electrode. In about half of the cells, the point of lowest threshold was found by searching with anodal current pulses; in the other cells, cathodal current pulses were used.

**Results.** Threshold measurements were obtained near the cell bodies of 20 ganglion cells and near the axons of 19 ganglion cells. Both cathodal and anodal stimuli evoked a neural response in the ganglion cells that consisted of a single action potential of near-constant latency that persisted when retinal synaptic transmission was blocked with cadmium chloride. For cell bodies, but not axons, thresholds for both cathodal and anodal stimulation were dependent on the search method used to find the point of lowest threshold. With search and stimulation of matching polarity, cathodal stimuli evoked a ganglion cell response at lower currents (approximately one seventh to one tenth axonal threshold) than did anodal stimuli for both cell bodies and axons. With cathodal search and stimulation, cell body median thresholds were somewhat lower (approximately one half) than the axonal median thresholds. With anodal search and stimulation, cell body median thresholds were approximately the same as axonal median thresholds.

**Conclusions.** The results suggest that cathodal stimulation should produce lower thresholds, more localized stimulation, and somewhat better selectivity for cell bodies over axons than would anodal stimulation. (*Invest Ophthalmol Vis Sci.* 2003; 44:3533–3543) DOI:10.1167/iovs.02-1041

Our ultimate goal is to develop an implantable retinal prosthesis that electrically stimulates the retina to provide some functional vision to patients with advanced retinitis pigmentosa or age-related macular degeneration. Retinitis pigmentosa and age-related macular degeneration are forms of blindness that result in substantial loss of photoreceptors. Although physiological and morphologic changes may take place in the inner retinas of affected patients,[1–5] the opportunity exists for direct electrical excitation of the residual neurons as a means of restoring vision.

Stimulation possibilities are either epiretinal (the stimulating points are on the inner surface of the retina) or subretinal (the stimulating points are on the outer surface of the retina, between the neural retina and the underlying pigment epithelium). The goal of the present study was to determine current threshold and increase in threshold with electrode displacement for epiretinal stimulation of retinal ganglion cells. The former can be used to judge the power requirements of a functioning prosthesis and the potential for electrochemical toxicity that occurs as current passes through the metal electrode. The latter can be used to guide the choice of interelectrode spacing and estimate the potential spatial resolution that could be derived from a prosthesis. Another motivation is the desire to achieve selective stimulation of ganglion cell bodies rather than axons en passage, which would presumably enhance the quality of perceptions induced by a retinal prosthesis.

Only a few studies[6–8] have been reported in which the currents needed to stimulate individual ganglion cells in the retina with an epiretinal electrode were investigated, and in none of these studies was the current thresholds of axons compared with cell bodies or the current thresholds measured as a function of electrode distance from the site of activation. Also, with the exception of Grumet et al.,[8] relatively large microelectrodes have been used in these studies. A small microelectrode was used in the present study to enable a more precise study of threshold variation with electrode position near a cell body or axon of a ganglion cell.

Preliminary portions of this work have been presented elsewhere[9] (Wyatt JL, et al. *IOVS* 1994;35:ARVO Abstract 593; Rizzo JF, et al. *IOVS* 1997;38:ARVO Abstract 182).

## Materials and Methods

Thirty-two adult New Zealand White rabbits (2–2.5 kg) were used in this study. All experimental procedures were in accordance with institutional guidelines and conformed to the guidelines of the ARVO Statement for the Use of Animals in Ophthalmic and Vision Research.

### Retinal Preparation

The rabbits were sedated by an intraperitoneal injection of urethane (1.6 g/kg) and then received an intravenous injection of pentobarbital sodium (20 mg/kg) for deep anesthesia. Under normal room lighting, an eye was enucleated and hemisected, and the vitreous humor was removed with gentle suction applied to the back of a Pasteur pipet. A strip ($\approx$1 $\times$ 2 cm) of inferior retina and attached sclera including the optic nerve head was removed and laid flat, ganglion cell side up, on a 10° inclined platform. The retinal strip was superfused with a solution of 8.9 g/L Ames medium (Sigma-Aldrich, St. Louis, MO), 1.9 g/L $NaHCO_3$, and 0.8 g/L D-glucose and saturated with 95% $O_2$-5% $CO_2$. The solution flowed by gravity over the surface of the retina at a rate of 1.4 to 1.7 mL/min. The temperature of the solution on the retina was maintained at 34°C to 36°C. Diffuse background light ($\approx$1 $\mu W/cm^2$ at the retina) was present throughout the experiments.

From [1]The Center for Innovative Visual Rehabilitation, VA Medical Center, Boston, Massachusetts; the [2]Department of Ophthalmology, Harvard Medical School and the Massachusetts Eye and Ear Infirmary, Boston, Massachusetts; and the [3]Research Laboratory of Electronics, Massachusetts Institute of Technology, Cambridge, Massachusetts.

Supported by grants from the VA Rehabilitation Research and Development Service (Project C-2726-C), the Foundation Fighting Blindness (T-VP-1000-69), and the Massachusetts Lions Club.

Submitted for publication October 9, 2002; revised March 4, 2003; accepted March 10, 2003.

Disclosure: **R.J. Jensen**, None; **J.F. Rizzo III**, None; **O.R. Ziv**, None; **A. Grumet**, None; **J. Wyatt**, None

The publication costs of this article were defrayed in part by page charge payment. This article must therefore be marked "*advertisement*" in accordance with 18 U.S.C. §1734 solely to indicate this fact.

Corresponding author: Ralph J. Jensen, The Center for Innovative Visual Rehabilitation, VA Medical Center, Mail Stop 151E, 150 South Huntington Avenue, Boston, MA 02130; ralph.jensen@med.va.gov.

## Electrical Recording and Stimulation

Extracellular potentials were recorded from ganglion cell axons by using standard glass-insulated tungsten microelectrodes.[10] Single-unit activity was amplified with a differential amplifier (DAM 80; World Precision Instruments, Sarasota, FL) with cutoff frequencies of 300 Hz and 10 kHz and displayed on an analog oscilloscope. The indifferent electrode was a 22-gauge needle electrically grounded to the retinal preparation.

The stimulating electrode was made of platinum and iridium with an exposed tip approximately 5 $\mu$m in length and 2 $\mu$m in diameter at the base (FHC Inc., Bowdoinham, ME; cat. 30-05-1). The small electrode area, smaller than one would perhaps expect to use in a prosthesis, enables a more precise study of threshold variation with electrode position near a cell body or axon. For stability, the shaft of the platinum-iridium electrode was surrounded by and glued to a concentric glass tube that extended to a point 6 mm short of the tip of the electrode. All stimuli in this study were monophasic, 100-$\mu$s duration, square-wave cathodal or anodal current pulses. The current pulses were generated by a calibrated stimulator (model S88; Grass Telefactor, Inc., W. Warwick, RI) and photoelectric stimulus isolation unit (model PSIU6; Grass Telefactor). The return electrode was a Ag-AgCl sheet (surface area: 1.2 $cm^2$) that lay on a platform beneath the sclera.

## General Experimental Protocol

The recording microelectrode was mounted on a micromanipulator and the microelectrode tip positioned above the retina several millimeters inferior to the optic nerve head. While lowering the microelectrode tip toward the surface of the retina, the experimenter intermittently stimulated the retina with light from a hand-held flashlight. Once action potentials from a single axon were isolated from background activity, the receptive field center of the ganglion cell was sought by flashing across the retina a 300-$\mu$m spot of light that was generated by an optical system described elsewhere.[11] After the center of the receptive field was located, the cell was physiologically categorized primarily on the basis of its response to flashes of light.[11] To simplify data analysis, only recordings from off-center, brisk-transient ganglion cells were selected for study. In addition, to avoid having the stimulus artifact (produced by the stimulating current) obscure the displayed evoked action potentials, only cells with receptive fields at least 6 mm from the recording electrode were studied.

Because the retinal strip lay on a 10° inclined platform, a 10° wedge was attached to the bottom of a second micromanipulator that held the stimulating electrode. This alignment insured that the plane of motion of the stimulating electrode tip matched the plane of the retinal surface. The *x*, *y*, and *z* spatial coordinates of the stimulating electrode were measured from three vernier micrometers on the micromanipulator.

Stimulation thresholds were determined by increasing a subthreshold current until action potentials were elicited more than 50% of the time over 10 or more consecutive stimulations. To aid detection of orthodromically generated action potentials, the oscilloscope sweep was pretriggered from the stimulator (Grass Telefactor). With few exceptions, only one ganglion cell was studied in each retinal strip. To minimize damage to the electrodes, currents greater than 300 $\mu$A were generally not used. The ability of the electrodes to pass current was routinely checked during the course of the study.

In some experiments, to block synaptic transmission within the retina, 1 mM cadmium chloride ($CdCl_2$; Sigma-Aldrich) was added to the bathing medium from a syringe pump, as described previously.[11]

## Specific Experimental Protocol

**Stimulation Near the Cell Body.** With the spot of light centered within the receptive field, the tip of the stimulating electrode was lowered in the bathing medium and positioned in the center of the spot. Alignment of the stimulating electrode over the receptive field center was facilitated by imaging with a video camera and displaying a 12× magnified view of the retina on a monitor. The spot was turned off and monophasic, square-wave current pulses (100 $\mu$s in duration, applied at 4–5 Hz) were delivered through the stimulating electrode. Stimulus current was continually adjusted as the electrode was slowly lowered toward the retina, and the physical point at which the threshold ceased to decline was taken to be the retinal surface.

In the search for the point of lowest threshold within the receptive field center, threshold measurements were first made along a line parallel to the *y*-axis extending ±150 $\mu$m from the center of the receptive field (Fig. 1). From the lowest threshold point found, a further search for the minimum was made along a line extending ±150 $\mu$m parallel to the *x*-axis. From this second minimum threshold point, a final search was conducted ±50 $\mu$m along a new line parallel to the *y*-axis. The point of lowest threshold found in the final search was used as the "measured origin," and all other electrode positions were plotted in relation to it. This tripartite search strategy was performed by using cathodal stimulation for half of the cells ($n = 10$) and anodal search for the other half ($n = 10$). Once the measured origin was determined for one polarity, the threshold to the opposite polarity was immediately determined without moving the electrode.

Thresholds at the retinal surface were then measured for six additional points separated by 50 $\mu$m along the *x*-axis and then six points along the *y*-axis. After each threshold determination, the microelectrode was raised 150 to 200 $\mu$m before the attempt was made to reposition it for the next measurement. Micrometer readings were used to guide relowering of the electrode to the presumed plane of the retinal surface. Finally, change in threshold as a function of distance above the measured origin (i.e., the *z*-axis, perpendicular to the retinal surface) was determined by measuring thresholds 25, 50, 75, 100, and 150 $\mu$m above the retina.

Much more dense measurements of current thresholds were made for one cell, for which the measured origin was found in an identical manner. In this case, 100 measurements were made at 25-$\mu$m increments in a 10 × 10 array in the *x*-*y* plane from the lowest threshold point found with anodal search. At all points, threshold-to-anodal current was first determined and then threshold to opposite polarity was immediately measured without moving the electrode.

**Stimulation Near the Axon.** To study axonal thresholds, the tip of a stimulating electrode was positioned at least 1.5 mm from the center of a ganglion cell's receptive field along an imaginary line connecting that center and the optic nerve head. Thresholds along axons were always studied below the visual streak, where axons are unmyelinated.

In the search for the point of lowest threshold, threshold measurements were first made along a line parallel to the *y*-axis (i.e., along a line perpendicular to the presumed course of the axon) extending ±150 $\mu$m. The point of lowest threshold was used as the measured origin, and all other electrode positions were plotted in relation to it. This search strategy was performed by using cathodal stimulation in 9 cells and anodal in 10 other cells. Once the measured origin was determined for one polarity, the threshold to the opposite polarity was immediately determined without moving the electrode. Thresholds at the retinal surface were then measured for six additional points separated by 50 $\mu$m along the *x*-axis and then six points along the *y*-axis. After each threshold determination, the microelectrode was raised 150 to 200 $\mu$m before attempting to reposition it for the next measurement. Finally, change in threshold as a function of distance above the measured origin (i.e., the *z*-axis) was determined by measuring thresholds 25, 50, 75, 100, and 150 $\mu$m above the retina.

## Statistical Methods

Medians (rather than means) are used to report data, primarily because they are much less sensitive to the effect of a small number of extreme outlying values. Medians are also helpful whenever high thresholds are reported as being simply greater than a certain value, as was done whenever it was judged that further elevation of current might damage the electrodes or cells. With such occasional semiquantitative results, medians but not means can still be accurately calculated.

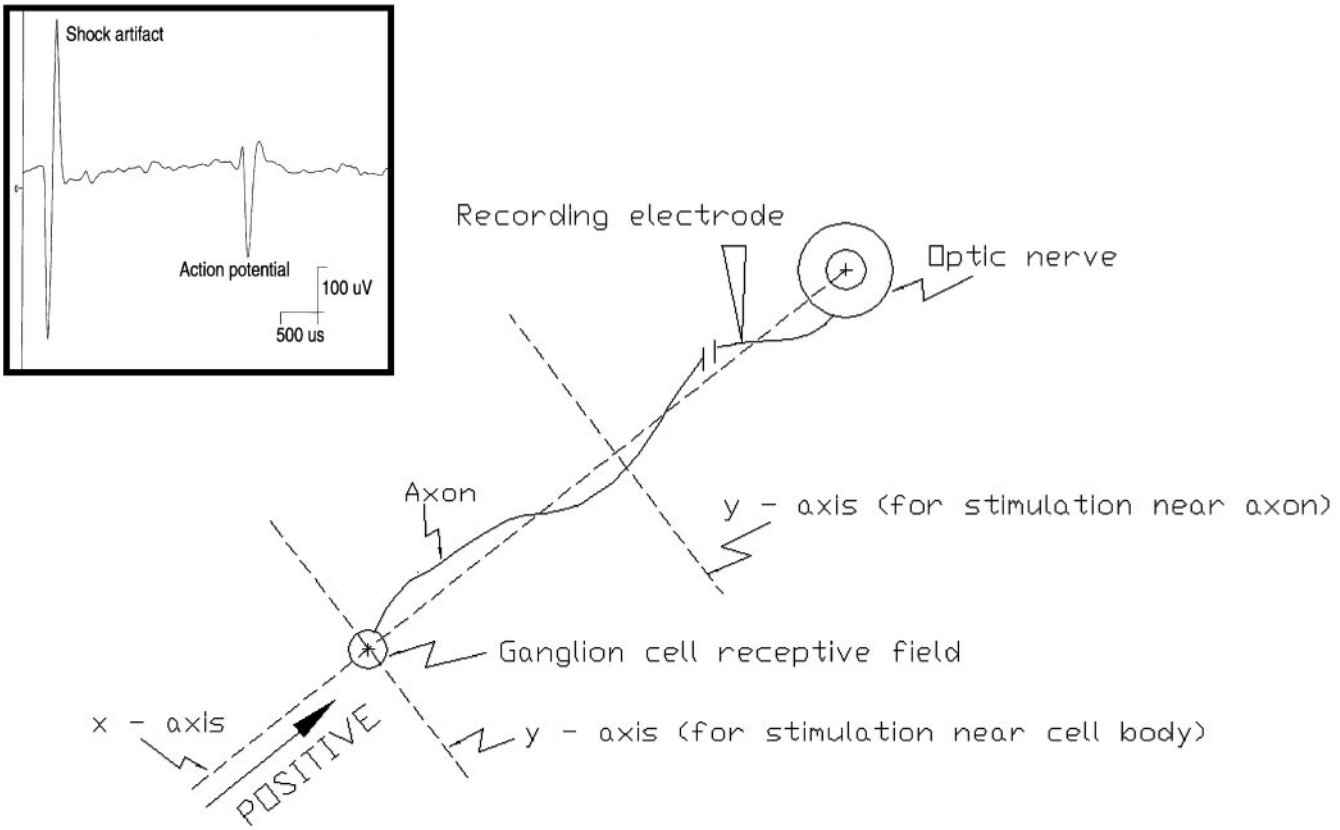


**FIGURE 1.** Orientation of *x* and *y* axes on the surface of the retina. With respect to the receptive field center of a ganglion cell, the *x*-axis was defined as being parallel to the presumed course of axons. The positive *x*-axis extends toward the optic nerve head. The *y*-axis was perpendicular to the *x*-axis. The waveform at *top left* gives an example of the stimulus shock artifact and an action potential recorded from the axon of a retinal ganglion cell.

## RESULTS

We report herein data obtained from 39 rabbit off-center brisk-transient ganglion cells in response to electrical stimulation. The data presented very likely derived from direct activation of the ganglion cells for several reasons: (1) near-constant latency at threshold stimulus intensity, (2) no marked reduction in latency at two to three times threshold intensities and (3) action potentials not abolished by bath addition of 1 mM cadmium chloride, a blocker of calcium-dependent synaptic transmission.

### Minimal Absolute Thresholds

**Stimulation Near the Cell Body.** Thresholds at the measured origin (see the Methods section for definition) within the receptive fields of 20 ganglion cells were plotted (Fig. 2A). In 10 cells, the measured origin was found with cathodal current pulses and in the other 10 with anodal current pulses. Thresholds for both cathodal and anodal stimulation were dependent on the search method used to find the measured origin. Median thresholds were lowest when the same polarity was used for search and stimulation. This was especially true of cathodal stimulation (median threshold obtained with cathodal search was one fourteenth that obtained with anodal search). Polarity-matched cathodal search and stimulation produced a narrow range of minimum thresholds (0.26–0.85 $\mu$A) with a median that was one tenth (0.50 vs. 5.0 $\mu$A) that of polarity-matched anodal search and stimulation.

**Stimulation Near the Axon.** Thresholds at the measured origin of 19 ganglion cell axons were also plotted (Fig. 2B). In 9 cells, the measured origin was found with cathodal current pulses and in the other 10 with anodal current pulses. Search polarity did not have a large effect on either the median cathodal or anodal thresholds. Polarity-matched cathodal search and stimulation produced minimum thresholds (from 0.50–3.2 $\mu$A) with a median that was one seventh (0.94 vs. 6.5 $\mu$A) that of polarity-matched anodal search and stimulation.

### Dense, Two-Dimensional Array of Threshold Measurements

**Stimulation Near the Cell Body.** A dense, two-dimensional array of threshold measurements in one ganglion cell, stimulated within the center of its receptive field, illustrates the dependence of threshold pattern on stimulus polarity (Fig. 3). This single difference in method produced an obviously lower and more highly localized minimum threshold for cathodal stimulation. Cathodal stimulation produced the lowest (0.18 $\mu$A) and highest (110 $\mu$A) thresholds.

A region of relatively low thresholds was evident from the center to upper right quadrant with both methods of stimulation. For cathodal stimulation, thresholds within this region were lower and those outside are higher than with anodal stimulation. One possible explanation for this area of low thresholds is that the axon of this ganglion cell emerged from this side of the cell body rather than the side of the cell body facing the optic nerve head (left in Fig. 3). This idea has support from anatomic studies.[12–14]

### Thresholds along the *x*-, *y*-, and *z*-Axes

**Stimulation Near the Cell Body.** Thresholds along the *x*-, *y*-, and *z*-axes in the 20 cells in Figure 2A were segregated by

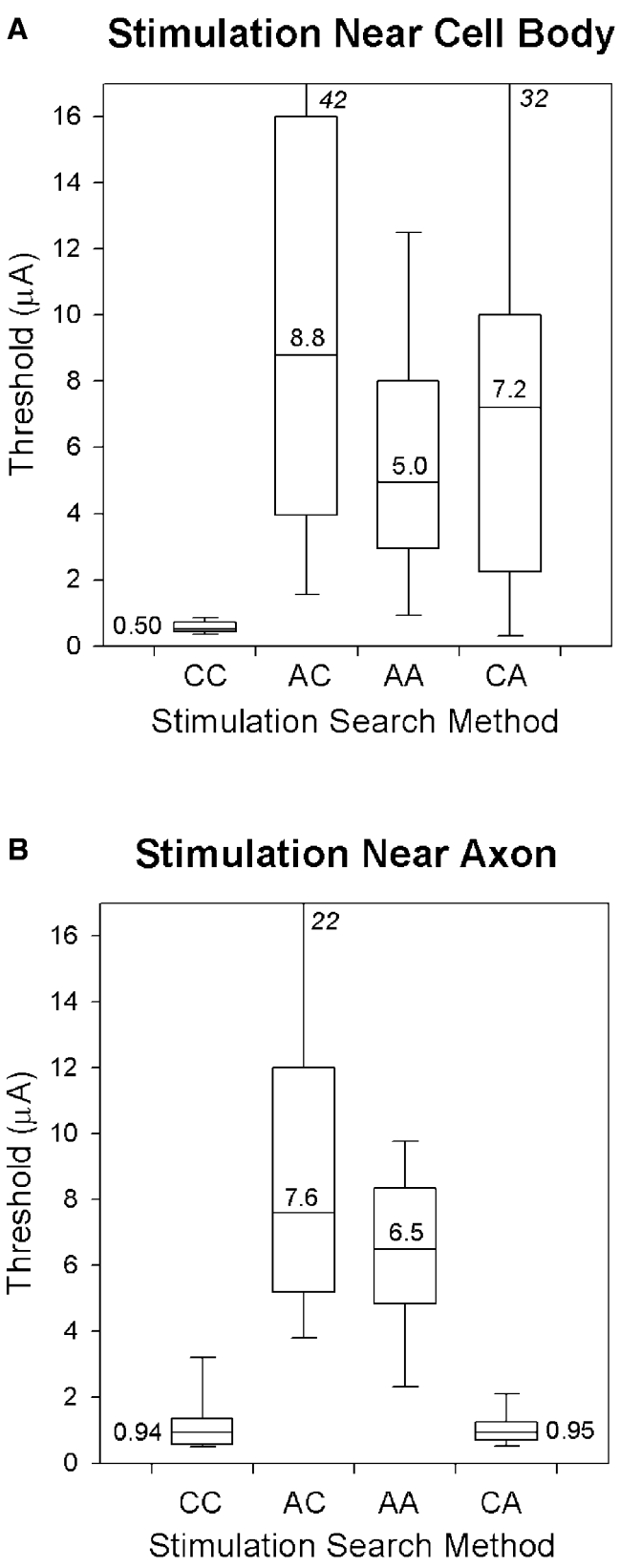


**FIGURE 2.** Current thresholds at the measured origin for stimulation near cell bodies (**A**) and near axons (**B**). The four stimulation search methods are cathodal stimulation after cathodal search (CC), anodal stimulation after cathodal search (AC), anodal stimulation after anodal search (AA), and cathodal stimulation after anodal search (CA). *Horizontal lines* bisecting the *vertical rectangles* (and the *numbers* immediately adjacent to these lines) represent the medians of the distributions. The *vertical rectangle* includes 50% of all measured thresholds. The *whiskers* attached to both ends of the *rectangles* extend to include 100% of the data. For clarity, the upper ends of three whiskers are not shown; the numbers in *italic* are the highest thresholds.

polarity of stimulation (Fig. 4A). The large spread in thresholds around the median was evident from the individual data, which were referenced to the linear axis. The semilog axis, in which vertical differences correspond to ratios of thresholds, expanded the lower range of thresholds and made evident the percentage increase in threshold with distance from the measured origin. The semilog plots emphasize the lower minimums and steeper percentage increase in thresholds around the measured origin with cathodal stimulation along the *x*- and *y*-axes. Recall from Figure 1 that the positive *x*-axis extended from the measured origin toward the optic nerve head, along the presumed path of the axon. The asymmetry of cathodal thresholds along the *x*-axis presumably resulted from stimulation of axons along the positive *x*-axis (Fig. 1).

**Stimulation Near the Axon.** Thresholds along the *x*-, *y*-, and *z*-axes of the 19 axons in Figure 2B were segregated by stimulus polarity (Fig. 4B). The spread in thresholds around the median is evident from the individual data, which were referenced to the linear axis. The median threshold scarcely varied with electrode displacement along the *x*-axis, which lay along the presumed path of the axon. Median cathodal thresholds are lower than median anodal thresholds at all locations. Cathodal thresholds also increased more rapidly, as a percentage, than anodal thresholds, with displacement from the measured origin along the *y*- and *z*-axes.

## Polarity of the Search Method

**Stimulation Near the Cell Body.** Figure 5A shows the data in Figure 4A separated by the polarity of the search method. For most positions of the stimulating electrode, thresholds were lower when the search and stimulation were polarity matched. Also, the lowest threshold in the vicinity of each cell body was found at the point revealed by the initial search to be the lowest threshold (i.e., the measured origin) when polarity-matched search and stimulation methods were used. This was not always true when the search and stimulation were of opposite polarity. The pairing between search and stimulation methods also had an effect on thresholds away from the measured origin. For polarity-matched methods, a 100-$\mu$m displacement of the electrode from the measured origin resulted in substantially greater relative increases in threshold for cathodal–cathodal than for anodal–anodal search and stimulation along all three axes. Similar to the more aggregated data in Figure 4A, the polarity-matched median threshold profiles along the *x*-axis were relatively symmetric with anodal, but not with cathodal, stimulation. This asymmetry results from the relatively slower increase in cathodal threshold from the measured origin to (+)150 $\mu$m, along the presumed axonal path (positive *x*-axis). Aggregated and polarity-matched cathodal methods both showed a deeper valley of thresholds around the measured origin along the *x*- and *y*-axes than the corresponding anodal method. Details of threshold increase with displacement are in Table 1.

We also examined the threshold profile of each cell along the *y*- and *z*-axes to determine how frequently the response plot of a single cell matches the shape of the median threshold profile derived from the aggregated data of all 20 cells. Along the *y*-axis, the expected U-shaped threshold profile was observed in 18 of the 20 cells with cathodal stimulation and in 15 of the 20 cells with anodal stimulation. In the other cells, an

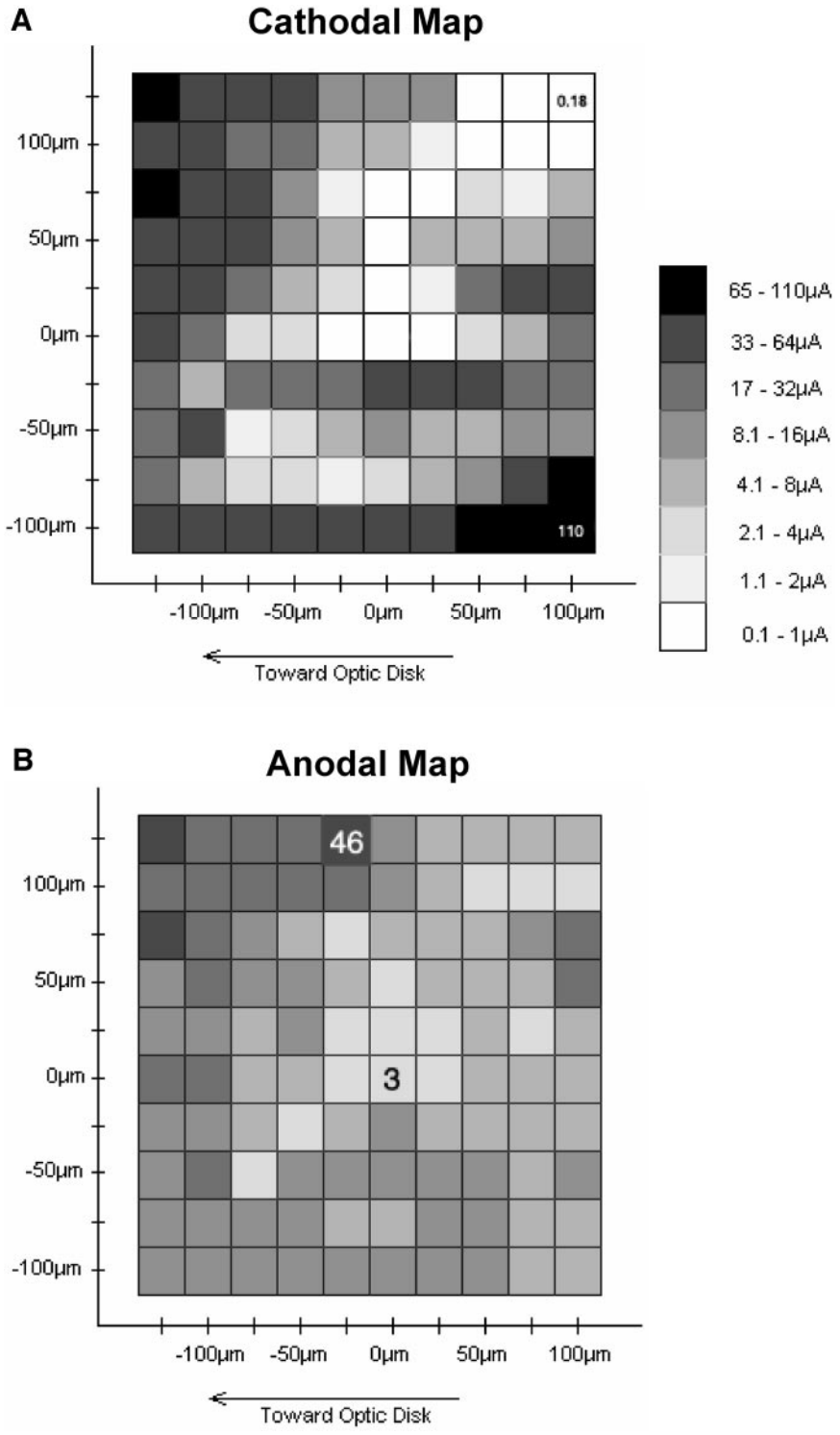


**FIGURE 3.** High spatial density thresholds in the *x-y* plane around one off-center brisk-transient retinal ganglion cell body. The measured origin was located by anodal search. Cathodal (**A**) and anodal (**B**) stimulation measurements were taken at 25-$\mu$m increments with the measured origin at the center. Thresholds are plotted using identical gray-scale values in both plots. The highest and lowest thresholds are given explicitly in both plots.

L-shaped profile was found (data not shown). A probable explanation for these L-shaped profiles is that the axon of these ganglion cells emerged from a site on the cell body other than the side of the cell body facing the optic nerve head. Along the *z*-axis, threshold profiles revealed a progressive increase with increasing displacement of the electrode from the retina in all 20 cases in which the search and stimulation were performed with the same polarity.

**Stimulation Near the Axon.** Figure 5B shows the separation of the data in Figure 4B by polarity of search method. The effect of search method was neither consistent nor dramatic. Matched search and stimulation yielded lower median thresholds in 14 of the 19 different electrode measurement sites with anodal stimulation, but in only 6 sites with cathodal stimulation. (Thresholds at the measured origin were determined once for the *x*- and *y*-axis plots and then redetermined for the *z*-axis plots.) For every axon, the lowest threshold turned out to lay either at the measured origin or along the *x*-axis. Details of threshold increase with electrode displacement are in Table 2.

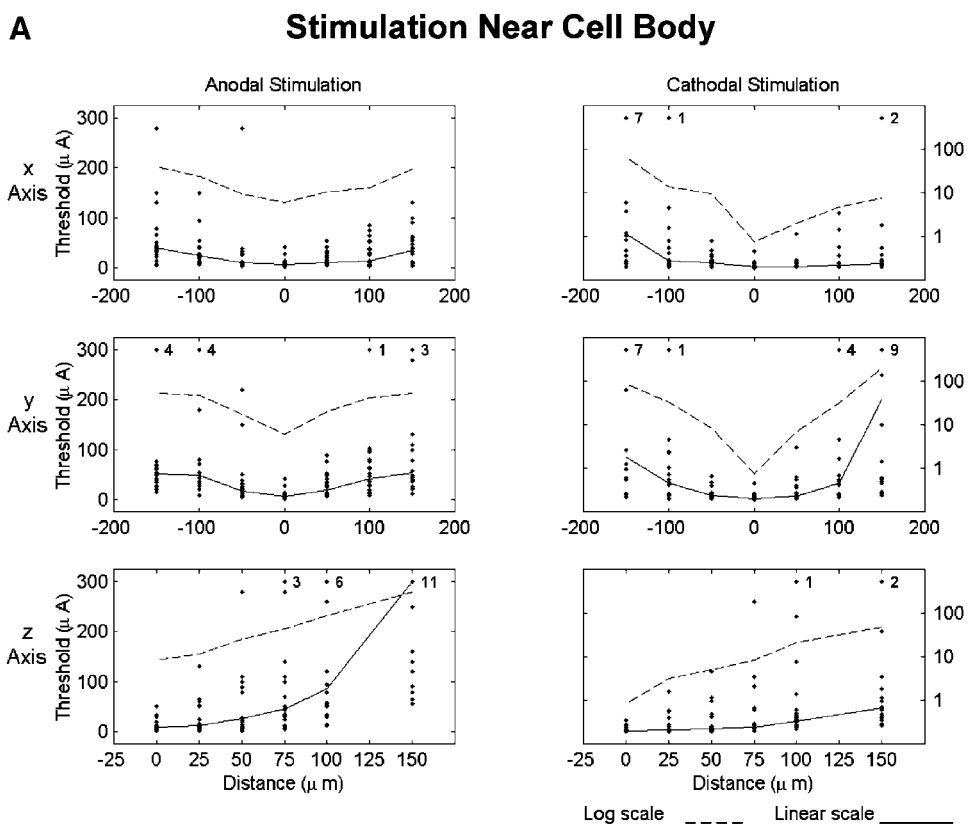


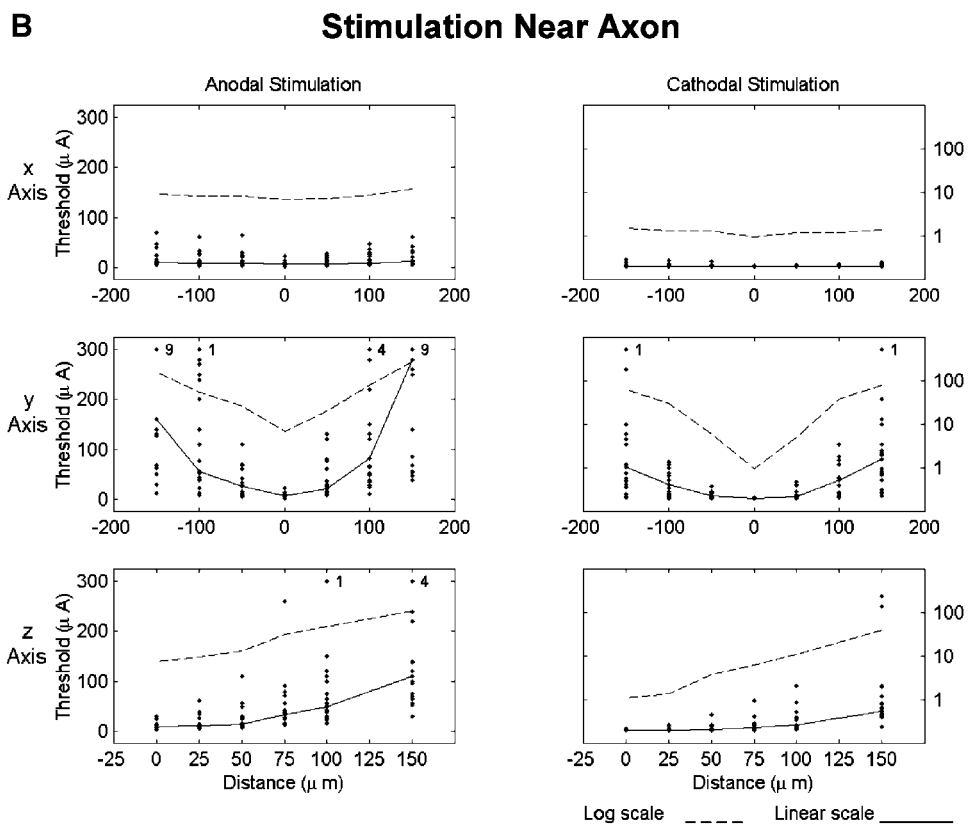


**FIGURE 4.** Current thresholds versus electrode displacement along *x*-, *y*-, and *z*-axes for stimulation near the (**A**) cell body and (**B**) axon for the same retinal ganglion cells as in Figure 2. Each data point indicates a threshold on the linear scale at *left*. The *numbers* next to the points along the uppermost division of the threshold axes are the number of thresholds that were 300 μA or greater. Thresholds obtained by anodal and cathodal search methods are combined in these plots. The results are separated by polarity of stimulation (anodal, *left*; cathodal, *right*). *Solid lines* connect median thresholds using the linear vertical axes on the *left*; *dashed lines* connect the same medians using the logarithmic axes on the *right*.

The lowest threshold minima and the steepest threshold profiles were obtained when cathodal stimulation was used (Figs. 2, 5, Table 2). At the measured origin, anodal stimulation with anodal search yielded thresholds that were approximately seven times greater than those found with cathodal stimulation. At this location, search polarity has no consistent effect

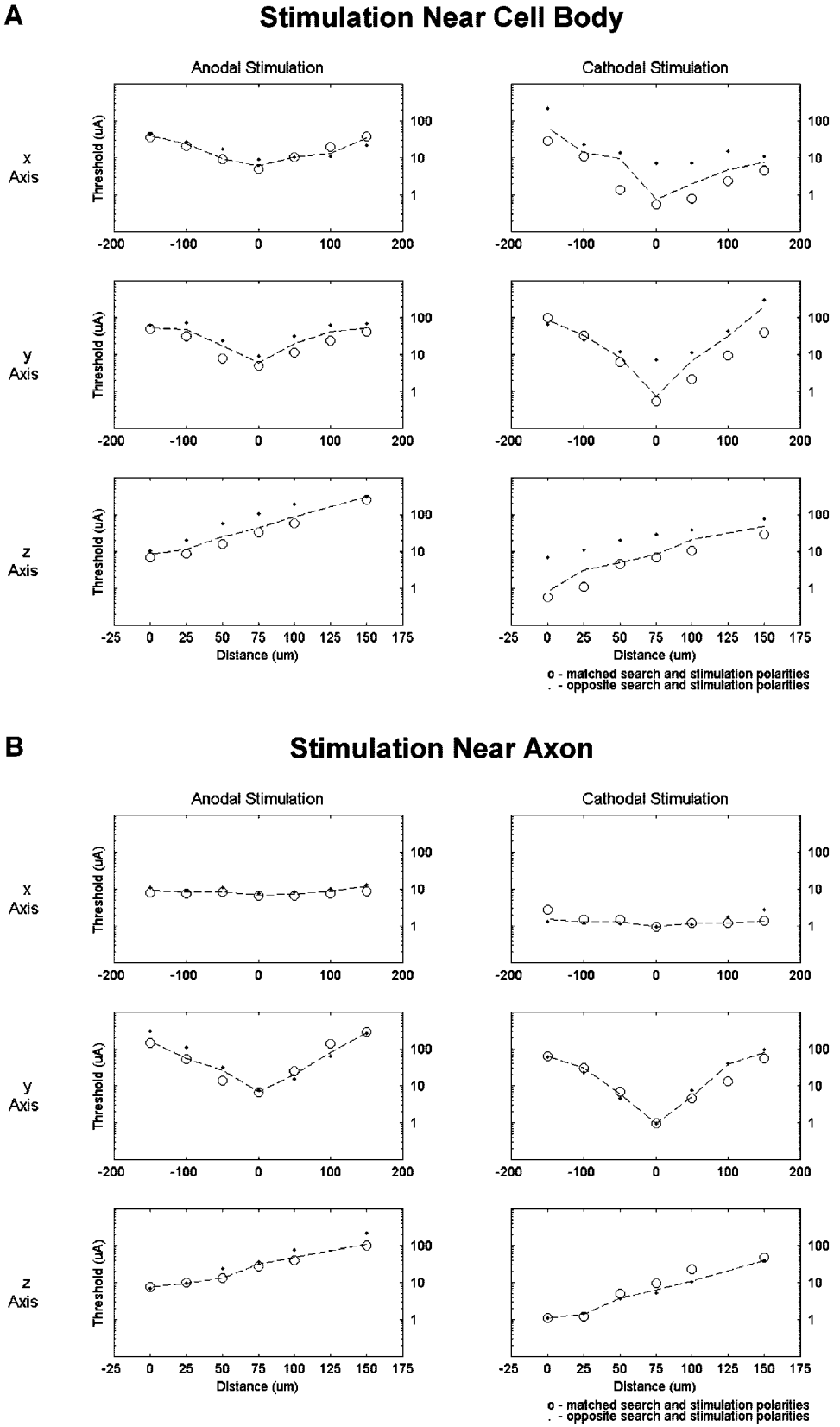


**FIGURE 5.** Semilog plots of the median thresholds in Figure 4, segregated by the polarity of the search method for stimulation near the (**A**) cell body and (**B**) axon. *Open circles*: median thresholds for polarity-matched search and stimulation; *dots*: thresholds found with the unmatched-polarity method. For comparison, *dashed lines* connect the same median values (combined by search method) as shown in Figure 4.

on threshold. With displacements of the stimulating electrode from the measured origin, anodal stimulation, preceded by a search of either polarity, produced higher thresholds than cathodal stimulation (Fig. 5). The difference (in percentage terms) decreased, however, the farther away the stimulating electrode was from the axon.

**TABLE 1.** Cell Body Threshold Summary

| Polarity of Search/Stimulation | Duration of Stimulation ($\mu$s) | Median Minimum Threshold ($\mu$A) | Ratio at 50 $\mu$m* | Ratio at 100 $\mu$m* |
|---|---|---|---|---|
| Cathodal–Cathodal | 100 | 0.50 | *x*: 2.6† | *x*: 20.0† |
| | | | *y*: 7.8‡ | *y*: 39.0‡ |
| | | | *z*: 7.9 | *z*: 18.1 |
| Anodal–Anodal | 100 | 5.0 | *x*: 1.8† | *x*: 4.2† |
| | | | *y*: 1.9‡ | *y*: 5.5‡ |
| | | | *z*: 2.3 | *z*: 8.1 |

* Ratio of median threshold at 50 (or 100) $\mu$m to median threshold at the measured origin (along the *x*-, *y*-, and *z*-axes).

† Data represent only the threshold at (−) 50 $\mu$m displacement ((−)100 $\mu$m in the last column).

‡ Data are the average increase at ±50 (or 100) $\mu$m.

## Power Fit to the Threshold Data

One simple hypothesis is that the electric field diminishes with the square of distance from the electrode during stimulation, as occurs in a uniform electrically linear medium with distant boundaries, and that thresholds increase accordingly. The hypothesis would imply, if true, that $I = kr^2$. The current threshold ($I$) rises as the square of distance ($r$). The coefficient $k$ characterizes the spread of the stimulating current. To compare the data with this hypothesis, we first normalized each measured threshold current, dividing it by the threshold measured for the same cell or axon at a 100-$\mu$m displacement in the same direction with the same stimulus polarity. (Only data obtained with search and stimulation of matching polarity were used. Data were excluded for electrode displacements along an axon (i.e., in the positive and negative $x$ directions for axonal stimulation and in the positive $x$ direction for cell body stimulation). Displacements in the positive and negative $y$ directions were lumped into a single category.)

The normalized thresholds were plotted and compared with square-law growth, which appears as a straight line on the log–log scale used. As a typical example, the normalized thresholds for anodal axon stimulation with electrode displacements in the $z$ direction (i.e., upward from the retinal surface) are plotted in Figure 6. Median thresholds fell less rapidly at displacements of 50 $\mu$m and lower from the measured origin than at larger displacements in Figure 6, and also in 7 other of the 10 categories shown in Figure 7. (The two exceptions were anodal thresholds in the $y$ direction for both cell bodies and axons.) For this reason we considered only the growth in threshold of displacements greater than 50 $\mu$m. The dashed line in Figure 6, corresponding to growth as the 1.78 power of displacement, gives the best fit on this log–log plot to the normalized thresholds for all displacements greater than 50 $\mu$m. (By "best fit," we mean the straight line on the log–log plot passing through unity at 100 $\mu$m that minimizes the sum of the squared differences between the logs of normalized thresholds at 75 and 150 $\mu$m and the log values on the straight line.) The advantage of fitting to the logarithm is that it gives equal weight to equal percentage deviations from square-law growth at 75 and 150 $\mu$m, despite the typically larger thresholds at the larger displacement.

Figure 7 illustrates the power law for threshold growth that best fits the log–log threshold plot for displacements greater

**TABLE 2.** Axonal Threshold Summary

| Polarity of Search/Stimulation | Duration of Stimulation ($\mu$s) | Median Minimum Threshold ($\mu$A) | Ratio at 50 $\mu$m* | Ratio at 100 $\mu$m* |
|---|---|---|---|---|
| Cathodal–Cathodal | 100 | 0.94 | *x*: 1.4x† | *x*: 1.4x† |
| | | | *y*: 6.0x† | *y*: 22.4x† |
| | | | *z*: 4.5x | *z*: 20.9x |
| Anodal–Anodal | 100 | 6.5 | *x*: 1.3x† | *x*: 1.2x† |
| | | | *y*: 3.0x† | *y*: 14.5x† |
| | | | *z*: 1.7x | *z*: 5.1x |

* Ratios are as in Table 1.

† Data are the average increase at ±50 (or ±100) $\mu$m.

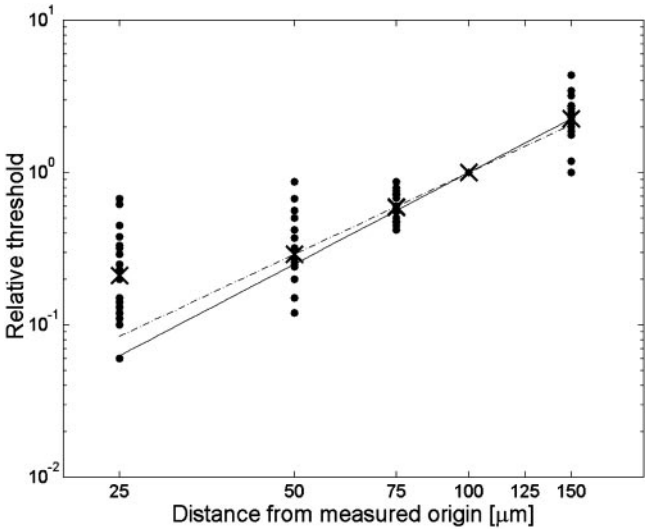


**FIGURE 6.** Normalized anodal axonal thresholds versus vertical displacement of electrode. For each axon, anodal current thresholds at each vertical (i.e., *z*-axis) displacement were normalized by dividing by the threshold measured at $z$ = 100 $\mu$m. Each *dot* represents one normalized threshold plotted on a log–log scale. (×) Median normalized threshold at each displacement. Threshold growth as a power of distance would appear as a straight line on these logarithmic axes. If thresholds increased with displacement squared, normalized thresholds would all lay along the *solid line*. *Dashed line*: best fit to the data at 75 and 150 $\mu$m of all straight lines passing through unity at 100 $\mu$m, representing thresholds growing as the 1.78 power of displacement.

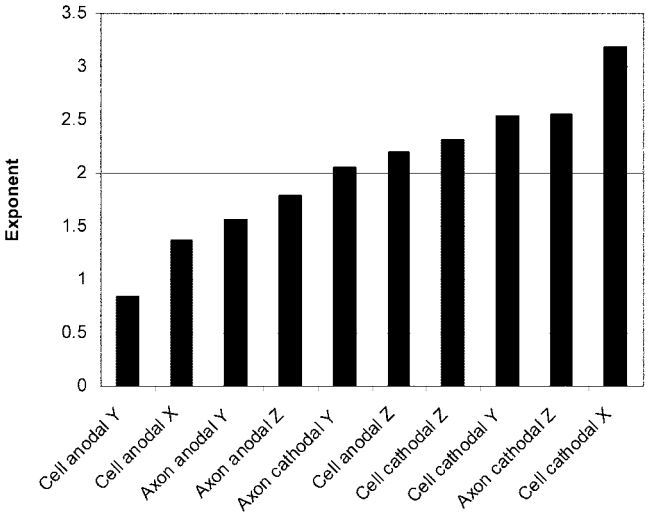


**FIGURE 7.** Power-law exponent for threshold growth with displacement for displacements greater than 50 $\mu$m, with polarity-matched search and stimulation.

than 50 μm in each category. These powers range from 0.84 to 3.19. Cathodal thresholds rise faster with displacement than anodal thresholds in every category. A similar distinction can be made across categories in most cases: of the 10 categories listed in Figure 7, the lowest four exponents are for anodal thresholds whereas the highest four are for cathodal. No systematic difference was found between the exponents for axons versus cell bodies.

### Effects of Cadmium Chloride

In this study, we found that electrical stimuli near threshold almost always evoked a single action potential, which was rigidly time locked to the electrical stimulus. Furthermore, there was a sharp stimulus threshold. Together, these findings indicate that the cells were directly stimulated. However, to be certain of this, for some cells we examined the thresholds to electrical stimulation when synaptic transmission in the retina was blocked. To block synaptic transmission, we applied 1 mM cadmium chloride in the bath for 5 minutes, which was a more than adequate time to abolish light responses from the ganglion cells. Thresholds were then remeasured without moving the stimulating electrode. Data were collected on 11 cells: In 8 cells, thresholds were measured with the stimulating electrode placed near the ganglion cell body; in the other 3 cells, thresholds were measured with the stimulating electrode placed near the axon. In no case did cadmium chloride abolish the electrically evoked action potentials. In six of the eight cells in which the stimulating electrode was placed near the cell body, the threshold current was elevated 11% to 23%. In one cell the threshold current remained unchanged, and in the other the threshold current decreased 32%. In all three cells in which the stimulating electrode was placed near the axon, the threshold current was elevated 8% to 35%. We attribute the small shifts in threshold to the direct, nonspecific effects of cadmium chloride.

## Discussion

In this study, we determined the current thresholds of off-center, brisk-transient ganglion cells in response to electrical stimulation with an ultrafine microelectrode placed near the axon or cell body. Undoubtedly, when the electrode was placed near the axon, the axon is the site of activation. However, when the electrode was placed near the cell body, the exact site of activation is questionable. Transsynaptic activation of cells was ruled out based on near-constant latency at threshold stimulus intensity, no marked reduction in latency at two to three times threshold intensity, and persistence of the electrically evoked response in the presence of the synaptic transmission blocker cadmium chloride. Parenthetically, transsynaptically evoked action potentials were clearly set up at currents much higher than the threshold currents for direct activation of ganglion cells, and these action potentials were abolished by addition of cadmium chloride to the bathing medium (Jensen RJ, unpublished observations, 2001). Recall from the Methods section that the stimulating electrode was positioned in the center of the receptive field of a ganglion cell and moved slightly from that point in search of the lowest threshold of current. The cell body, axon, or any one of the dendrites could be the site of activation. In experimental studies conducted in other areas of the central nervous system, the minimum threshold point was determined to be at the initial segment of the axon.[15–17] For ease of discussion, herein we use the term cell body stimulation to refer to stimulation with an electrode placed in the center of the receptive field of a ganglion cell.

### Minimal Absolute Thresholds

As summarized in Figure 2, both cell bodies and axons are more sensitive to cathodal stimulation than anodal stimulation. This finding was not unexpected; it has long been known that cathodal currents are more effective than anodal currents in stimulating neurons within the central nervous system.[18–20] Figure 2 also shows that the minimum absolute threshold for cell body stimulation was dependent on the polarity of current used to search for the minimum threshold point. This was particularly true of thresholds obtained with cathodal stimulation—the median threshold after cathodal search was approximately 14 times lower (0.50 vs. 7.2 μA) than the median threshold after anodal search. In comparison, the median threshold for cathodal stimulation of axons after cathodal search was virtually the same (0.94 vs. 0.95 μA) as that after anodal search. Why should the polarity of current used to search for the minimum threshold point matter in cell bodies but not in axons?

On the one hand, cathodal stimulation of any excitable cell is readily explained by direct depolarization of the cell in the region under the electrode. Anodal stimulation, on the other hand, results in hyperpolarization of the cell in the region under the electrode. To explain anodal stimulation it has been proposed that current leaves (and depolarizes) sites distant from the electrode.[15] Consequently, the site of lowest threshold for anodal stimulation may be different from the site of lowest threshold for cathodal stimulation. This was clearly the case when a dense, two-dimensional array of threshold measurements was made near the cell body of one ganglion cell (Fig. 3). For this cell, the measured origin was located using anodal search and the site of lowest threshold for cathodal stimulation was located approximately 150 μm from the measured origin. Whereas a retinal ganglion cell has a complex geometry in the area of its receptive field, an intraretinal axon is essentially a uniform, one-dimensional structure. Consequently, the point of minimum threshold of an axon is not a single point but a series of points along its length. Whether the region of depolarization is under the electrode (cathodal stimulation) or at a site distant from the electrode (anodal stimulation) should be inconsequential in locating a minimum threshold point.

Another finding from the data presented in Figure 2 is that with matched-polarity cathodal search and stimulation, the median threshold for cell body stimulation was approximately one half (0.50 vs. 0.94 μA) that of axonal stimulation when the stimulating electrode was at the measured origin. With matched-polarity anodal search and stimulation, the median threshold for cell body stimulation was nearly the same as that of axonal stimulation (5.0 vs. 6.5 μA). Thus, with cathodal current, it appears possible to stimulate cell bodies preferentially. That is, if an electrode is placed on an arbitrary patch of retina containing axons and cell bodies, cells with initial segments that are directly under the electrode will be activated first. It is noteworthy that several years ago Greenberg et al.[21] had predicted based on a computational model of electrical stimulation of retinal ganglion cells that it should be possible to stimulate retinal ganglion cells electrically near the cell body at lower thresholds than at the axon.

### Thresholds along the *x*-, *y*-, and *z*-Axes

Median cathodal thresholds were lower than median anodal thresholds in both cell bodies and axons at almost every displacement (Figs. 4, 5). Median axonal thresholds increased more rapidly with displacement in the *y* and *z* directions under cathodal stimulation than under anodal stimulation (Fig. 4B). Similar behavior was noted in cell bodies (Fig. 4A). We also found that with matched-polarity cathodal search and stimula-

tion, median axonal thresholds generally increased less steeply with displacement than cell body thresholds. (The one slight exception being *z*-axis thresholds at 100 μm.) With matched-polarity anodal search and stimulation, however, no consistent difference in steepness between cell bodies and axons was found (Tables 1, 2).

We found that the median axonal thresholds scarcely changed with displacement in *x*-axis under either cathodal or anodal stimulation (Figs. 4B, 5B, Table 2). This finding is reassuring from a technical standpoint because this axis presumably lies along the path of the axon. The median cell body thresholds did not increase as steeply along the positive *x*-axis as it did along the negative *x*-axis (Figs. 4A, 5A). In most ganglion cells, the axon would have presumably coursed along the positive *x*-axis.

For application to a retinal prosthesis, two important points to be made are that both cell bodies and axons are more sensitive to cathodal than to anodal stimulation, even at distances far removed from the point of lowest threshold, and that cathodal current should provide a more focal stimulation of the retina.

## Polarity of the Search Method

The search polarity had little effect on axonal thresholds at most displacements in distinct contrast to the cell body's great sensitivity to search polarity (Fig. 5). This finding suggests that the location of the measured origin is more or less independent of the search method for an axon, whereas this is not true for the cell body.

## Power Fit to the Threshold Data

The threshold for electrical stimulation of neurons with an extracellular microelectrode has generally been considered to vary with the square of the distance between the neuron and the electrode tip (see review by Tehovnik[22]). We found though that the threshold's increase with distance is not accurately described by a radius (r)-squared law. A best fit to the data gives a power law ranging from $r^{0.84}$ to $r^{3.19}$ (Fig. 7). Thresholds declined more slowly than $r^2$ as distance was reduced from 50 to 25 μm (e.g., Fig. 6). No systematic difference was found between the exponents for axons and cell bodies. A mathematical model to explain why our data cannot be described by a radius-squared law is currently being developed in our laboratory.

## Comparison with Previous Studies

Although the retina has been electrically stimulated in several studies, we are aware of only three studies[6–8] in which the minimum currents needed to activate individual retinal ganglion cells with an epiretinal electrode have been investigated. The first study, by Crapper and Noell,[6] recorded the responses of rabbit retinal ganglion cells to electrical stimuli (0.5-ms cathodal and anodal pulses) delivered from a 100-μm steel needle electrode. They found that ganglion cells produce one or more bursts of action potentials on electrical stimulation. They supposed that photoreceptors, not ganglion cells, are the primary site of activation for the burst of action potentials. They also mentioned that with a strong electrical stimulus an "immediate" response could be seen, which they attributed to direct stimulation of ganglion cells. In contrast to their findings, we found that the threshold current for direct stimulation of ganglion cells is lower than that needed to generate a delayed burst of spikes at the 100-μs duration we used. Bursts of spikes were observed with currents considerably above the threshold for direct stimulation (Jensen RJ, unpublished observations, 2001). We believe this difference in our findings and theirs may be due to the differences in the electrode size and pulse duration.[23]

Humayun et al.[7] stimulated the inner retinal surface of rabbits and bullfrogs with biphasic current pulses (75-μs phase duration) from a relatively large (200-μm diameter) spherical electrode. They found that responses were recordable in ganglion cells with currents as low as 50 μA. The responses exhibited a short latency, suggesting direct stimulation of the ganglion cells. That they needed approximately 100 times more current to activate a ganglion cell is not surprising because of the large size of the electrode and hence the reduced charge density. They did not report observing bursts of spikes at longer latencies, which is not surprising because they used a short pulse duration in their study. Short pulse durations appear to be ineffective in activating preganglionic neurons in frog[24] and rabbit retinas.[23]

Grumet et al.[8] stimulated rabbit retinal ganglion cells with biphasic current pulses from a microelectrode array of 10-μm-diameter disc electrodes. They reported that threshold currents in the cells in their study were all below 2 μA with axonal stimulation. In our study, we found that the threshold currents with axonal stimulation were all below the 3.2 μA with monophasic cathodal stimulation (Fig. 2). Such close agreement between their results and ours is probably due to the relatively similar size of electrodes in both studies, although the surface area of their disc electrode (79 $\mu m^2$) is approximately five times the surface area of our cone-shaped electrode (16 $\mu m^2$). Because of limitations in their experimental setup, they were not able to investigate the amount of current needed to stimulate a ganglion cell near its cell body, and therefore no comparisons can be made for cell body stimulation.

## Applicability of Results to a Retinal Prosthesis

The electrodes used had an exposed area that was conical in shape: 5 μm long and 2 μm in diameter at the base. These small electrodes were chosen to give a more accurate indication of threshold variation with displacement near a cell body or axon than could be obtained with the much larger electrodes typically considered for a retinal implant (e.g., 400-μm-diameter discs).[25,26] The small size resulted in an average charge density of 0.63 millicoulombs/$cm^2$ for a 1-μA, 100-μs pulse, which is near the maximum charge density recommended for safe prolonged stimulation (e.g., 2–4 mC/$cm^2$ for iridium oxide[27] and 0.3–0.4 mC/$cm^2$ for platinum[28]). At 100 μm displacement, the charge density at median threshold would exceed the upper limit for iridium oxide. Furthermore, because current is known to concentrate at the tip of such pointed electrodes, the peak charge density is doubtless greater by an unknown amount.

It is reassuring that similarly low-current thresholds are obtained for rabbit retinal ganglion cell axons with 10-μm-diameter disc electrodes,[8] which presumably produce a charge density at least five times less than our electrode. It remains to be determined whether ganglion cell bodies have a lower threshold to cathodal stimulation with these disc electrodes, as we have found in the present study with our cone-shaped microelectrode.

## *References*

1. Santos A, Humayun M, S de Juan E, et al. Preservation of the inner retina in retinitis pigmentosa: a morphometric analysis. *Arch Ophthalmol.* 1997;115:511–515.
2. Stone JL, Barow WE, Humayun MS, de Juan E, Milam AH. Morphometric analysis of macular photoreceptors and ganglion cells in retinas with retinitis pigmentosa. *Arch Ophthalmol.* 1992;110:1634–1639.
3. Fariss RN, Li Z-Y, Milam AH. Abnormalities in rod photoreceptors, amacrine cells, and horizontal cells in human retinas with retinitis pigmentosa. *Am J Ophthalmol.* 2000;129:215–223.

4. Medeiros NE, Curcio CA. Preservation of ganglion cell layer neurons in age-related macular degeneration. *Invest Ophthalmol Vis Sci.* 2001;42:795–803.
5. Strettoi E, Porciatti V, Falsini B, Pignatelli V, Rossi C. Morphological and functional abnormalities in the inner retina of the rd/rd mouse. *J Neurosci.* 2002;22:5492–5504.
6. Crapper DR, Noell WK. Retinal excitation and inhibition from direct electrical stimulation. *J Neurophysiol.* 1963;26:924–947.
7. Humayun M, Propst R, de Juan E, McCormick K, Hickingbotham D. Bipolar surface electrical stimulation of the vertebrate retina. *Arch Ophthalmol.* 1994;12:110–116.
8. Grumet AE, Wyatt JL, Rizzo JF. Multi-electrode stimulation and recording in the isolated retina. *J Neurosci Methods.* 2000;101:31–42.
9. Jensen RJ, Rizzo JF, Grumet AE, Edell DJ, Wyatt JL. *Single Unit Recording Following Extracellular Electrical Stimulation of Rabbit Retinal Ganglion Bodies.* Technical Report 600, Cambridge, MA: MIT Research Laboratory of Electronics; 1996.
10. Levick WR. Another tungsten microelectrode. *Med Biol Eng.* 1972; 10:510–515.
11. Jensen RJ. Mechanism and site of action of a dopamine $D_1$ antagonist in the rabbit retina. *Vis Neurosci.* 1989;3:573–585.
12. Amthor FR, Oyster CW, Takahashi ES. Quantitative morphology of rabbit retinal ganglion cells. *Proc R Soc Lond B.* 1983;217:341–355.
13. Peichl L, Buhl, EH, Boycott, BB. Alpha ganglion cells in the rabbit retina. *J Comp Neurol.* 1987;263:25–41.
14. Kolb H, Linberg KA, Fisher SK. Neurons of the human retina: a Golgi study. *J Comp Neurol.* 1992;318:147–187.
15. Ranck JB. Which elements are excited in electrical stimulation of mammalian central nervous system: a review. *Brain Res.* 1975;98: 417–440.
16. Gustafsson B, Jankowska E. Direct and indirect activation of nerve cells by electrical pulses applied extracellularly. *J Physiol.* 1976; 258:33–61.
17. Nowak LG, Bullier J. Axons, but not cell bodies, are activated by electrical stimulation in cortical gray matter. I. Evidence from chronaxie measurements. *Exp Brain Res.* 1998;118:477–488.
18. Porter R. Focal stimulation of hypoglossal neurones in the cat. *J Physiol.* 1963;169:630–640.
19. BeMent SL, Ranck JB. A quantitative study of electrical stimulation of central myelinated fibers. *Exp Neurol.* 1969;24:147–170.
20. Stoney SD, Thompson, WD, Asanuma H. Excitation of pyramidal tract cells by intracortical microstimulation: effective extent of stimulating current. *J Neurophysiol.* 1968;31:659–669.
21. Greenberg RJ, Velte TJ, Humayun MS, Scarlatis GN, de Juan E. A computational model of electrical stimulation of the retinal ganglion cell. *IEEE Trans Biomed Eng.* 1999;46:505–514.
22. Tehovnik EJ. Electrical stimulation of neural tissue to evoke behavioral responses. *J Neurosci Methods.* 1996;65:1–17.
23. Jensen RJ, Ziv OR, Rizzo JF. Stimulation of ganglion cells in rabbit retina with a microelectrode placed on the inner retinal surface. *Proceedings of the Rehabilitation Research and Development 3rd National Meeting*. Department of Veterans Affairs, Arlington, VA. 2002:92. http://www.vard.org/va/02/meet02.htm. Accessed 2002.
24. Greenberg RJ, Humayun MS, de Juan E. Selective stimulation of retinal subgroups by varying electrical pulse duration (Abstract). *Soc Neurosci Abstr.* 1997;23:919.2.
25. Humayun MS, de Juan E, Weiland JD, et al. Pattern electrical stimulation of the human retina. *Vision Res.* 1999;39:2569–2576.
26. Rizzo JF, Wyatt J, Loewenstein J, Kelly S, Shire D. Methods and perceptual thresholds for short-term electrical stimulation of human retina with microelectrode arrays. *Invest Ophthalmol Vis Sci.* In press.
27. Beebe X, Rose TL. Charge injection limits of activated iridium oxide electrodes with 0.2 ms pulses in bicarbonate buffered saline. *IEEE Trans Biomed Eng.* 1988;35:494–495.
28. Brummer SB, Turner MJ. Electrical stimulation with Pt electrodes II: estimation of maximum surface redox (theoretical nongassing) limits. *IEEE Trans Biomed Eng.* 1977;24:440–443.